X-621-69-88
PREPRINT

THE THERMOSPHERIC TIDES AS AN OSCILLATOR CIRCUIT SYSTEM

H. VOLLAND

MARCH 1969

GODDARD SPACE FLIGHT CENTER
GREENBELT, MARYLAND

X-621-69-88
Preprint

THE THERMOSPHERIC TIDES AS AN OSCILLATOR CIRCUIT SYSTEM

H. Volland*

March 1969

*NAS/NRC research associate, now at the Astronomical Institutes of the University in Bonn, Germany.

GODDARD SPACE FLIGHT CENTER
Greenbelt, Maryland

THE THERMOSPHERIC TIDES AS AN OSCILLATOR CIRCUIT SYSTEM

H. Volland

ABSTRACT

The in situ generation of neutral air waves within the thermosphere by an external heat source is calculated using an approximate approach where the density amplitude represents the electric current and the heat source replaces the electric voltage. The energy equation can be transformed in such a way that it formally is equivalent to the equation of an electric circuit system in series by neglecting the transmission quality of the waves. The "inductance" of the circuit is related to internal heat of the wave and to vertical heat convection, the "capacitance" is related to horizontal and vertical heat convection and the "resistance" is related to ion drag and vertical heat conduction. Numerical calculations depending on frequency, collision number and horizontal wave number agree sufficiently well with exact full wave calculations. They are applied to the diurnal and semidiurnal tidal density variations, to the geomagnetic activity effect, the 27 day variation and the semiannual effect within thermospheric heights.

THE THERMOSPHERIC TIDES AS AN OSCILLATOR CIRCUIT SYSTEM

1. INTRODUCTION

Within the thermosphere the diurnal component of the tidal wave predominates the density variations. This tidal wave is generated by solar EUV heat input within the thermosphere on the one hand and by a diurnal tidal gravity wave from the lower atmosphere on the other hand (Volland, 1968). Above 300 km altitude the EUV generated tidal wave dominates. The observations show maximum density between 14^{00} and 15^{00} local time. The maximum is delayed by 2 to 3 hours with respect to the solar EUV heat input which has its maximum at 12^{00} local time (see e.g., Priester et al., 1967). It has been shown that this time delay is the natural response time of the thermospheric circuit system with respect to the generating heat source (Volland, 1968).

We will give in this paper a simplified derivation of the diurnal tidal density wave within the thermosphere. We shall compare it with an electric network driven by an alternative voltage generator. We shall find complete equivalence between both systems. We therefore can define an atmospheric "condensor", "inductor" and "resistor" equivalent to heat convection, internal energy and heat conduction and ion drag, respectively. The amplitude and phase relationship between atmospheric "current" (density) and atmospheric "voltage" (heat source) and its dependence on the atmospheric "circuit elements" can be determined. This equivalence not only is valid for the diurnal period but generally for atmospheric disturbances of sinusodial form at thermospheric heights.

2. THE ELECTRIC CIRCUIT SYSTEM

An electric circuit system in series consisting of inductance L, capacitance C and resistance R driven by an alternative voltage generator of voltage u (see Figure 1) has the well known relationship between electric current i and electric voltage u of

$$i = \frac{u_0}{Z} e^{j\omega t - j\Phi} \tag{1}$$

where u_0 is the amplitude and ω is the angular frequency of the driving alternative voltage generator, t is the time,

$$Z = \sqrt{\left(\omega L - \frac{1}{\omega C}\right)^2 + R^2} \tag{2}$$

is the impedance and

$$\Phi = tg^{-1}\left[\frac{\left(\omega L - \frac{1}{\omega C}\right)}{R}\right] \tag{3}$$

is the phase delay between current i and voltage u (see e.g., Glasford, 1965).

Current and voltage are in phase if the frequency ω equals the eigenfrequency Ω of the system:

$$\omega = \Omega = \frac{1}{\sqrt{LC}} \tag{4}$$

The current i is delayed by 90° if R = 0 and $\omega > \Omega$. i shows a phase advance of 90° with respect to u if R = 0 and $\omega < \Omega$.

3. THE ATMOSPHERIC CIRCUIT SYSTEM

We now shall derive a completely equivalent formula for the diurnal tidal thermospheric density wave $\Delta\rho$ generated by a heat input Δq. We consider the thermosphere as a circuit system in which energy is provided via direct EUV heat input Δq. Strictly speaking the thermosphere behaves like a transmission system of four port quality. Waves generated outside the thermosphere (the tidal wave from the lower atmosphere) propagate through the thermosphere with finite phase velocity and with finite attenuation rate. Waves generated at a certain place within the thermosphere (e.g., by EUV heating) propagate out of the thermosphere and contribute to the diurnal density variation not only at the place of their generation but throughout the whole thermosphere. In the height range between 300 and 400 km, which we shall consider exclusively, the tidal wave from below still contributes significantly to the density variation. In our approximation we neglect the transmission line quality of the thermosphere and consider only the in situ generation of the waves without taking into account their propagation characteristics.

We consider a two dimensional model of an isothermal thermosphere and a heat input harmonic in local time τ and exponentially decreasing with height z:

$$\Delta q = \Delta q_0 \, e^{j\,\omega\tau - (z - z_0)/H} \tag{5}$$

with

$$\omega\tau = \omega t + k_y y .$$

ω is the angular frequency of the earth's rotation, y is the coordinate along the equator (positive in east direction), z is the altitude, $k_y = 1/a$ is the horizontal wave number (a is the earth's radius), H is a scale height and z_0 is a reference height. From the equations of conservation of mass, momentum and energy and from the equation of state we can derive the following expressions (see e.g., Volland, 1969a)

$$j\omega\Delta\rho + \rho_0 \frac{\partial \Delta w}{\partial z} + j k_y \rho_0 \Delta v - \frac{\rho_0}{H_0} \Delta w = 0 \qquad (6a)$$

$$j\omega\rho_0 \Delta v + \nu \rho_0 \Delta v + j k_y \Delta p = 0 \qquad (6b)$$

$$\frac{\partial \Delta p}{\partial z} + g\Delta\rho = 0 \qquad (6c)$$

$$j\omega c_v \rho_0 \Delta T + j k_y p_0 \Delta v + p_0 \frac{\partial \Delta w}{\partial z} - \frac{\partial}{\partial z}\left(\kappa_0 \frac{\partial \Delta T}{\partial z}\right) = \Delta q \qquad (6d)$$

$$\frac{\Delta p}{p_0} = \frac{\Delta\rho}{\rho_0} + \frac{\Delta T}{T_0} \qquad (6e)$$

It is

ρ_0, T_0, p_0 mean values of density, temperature and pressure

$\Delta\rho$, ΔT, Δp wave parameters of density, temperature and pressure

Δv, Δw horizontal wind (positive in east direction) and vertical wind

ν collision number between the ions and one neutral

g magnitude of the gravitational acceleration force

c_v specific heat at constant volume

κ_0 coefficient of mean heat conductivity

H_0 scale height of the isothermal thermosphere.

In the equation of conservation of vertical momentum (6c) we neglected the vertical velocity and in the equation of conservation of energy (6d) we neglected the horizontal heat flux, because both terms are small compared with the vertical pressure gradient and the vertical heat flux, respectively. Since the wave propagation is considered to take place at low latitudes from west to east, the Coriolis force is small and can be neglected, too, in the equation of conservation of horizontal momentum (6b). Furthermore, in Equation (6b) we ignored molecular viscosity which gives rise to a term on the left side in Equation (6b) of

$$-\eta\left(\frac{\partial^2 \Delta v}{\partial z^2} - k_y^2 \Delta v\right) \tag{7}$$

where η is the coefficient of molecular viscosity.

From our approach given below we can estimate the magnitude of this term as compared with the ion drag term $\nu \rho_0 \Delta v$. At 350 km altitude using reasonable numerical data we find that the viscosity term is only a fraction of the ion drag term and can be considered to be included within an effective collision number ν.

The energy equation (6d) is in fact the first law of thermodynamics. The respective terms on the left hand side of Equation (6d) represent therefore the change of the internal energy of the gas, horizontal and vertical heat convection (the work done by the gas) and vertical heat conduction considered as an external heat sink, while the right hand side gives the change of the external

heat input. We shall make use of these expressions throughout the following sections.

From an exact treatment of the complete system Equation (6) it can be shown (Volland, 1968) that $\Delta\rho$, Δp and $\kappa_0 \frac{\partial \Delta T}{\partial z}$ are nearly in phase and that their height dependence in the height range between 300 and 400 km can fairly well be described by exponential expressions:

$$\left.\begin{matrix}\Delta\rho \\ \Delta p \\ \kappa_0 \Delta T'\end{matrix}\right\} \sim \left\{\begin{matrix}\Delta\rho_0 \\ \Delta p_0 \\ \kappa_0 \Delta T_0'\end{matrix}\right\} e^{-(z-z_0)/H_1} \qquad (8)$$

H_1 is a scale height and z_0 is the same reference height as in Equation (5). $\Delta\rho_0$, Δp_0 and $\kappa_0 \Delta T_0'$ are related to this height. (For abbreviation we replaced the height derivative by a prime:

$$\frac{\partial}{\partial z} = ').$$

The absence of an imaginary term in the exponents of Equation (8) indicates the quasi-evanescent behavior of the tidal wave at those heights which is due to the dominant influence of heat conduction.

Because we assume an isothermal thermosphere it is

$$\left.\begin{matrix}\rho_0 \\ \\ p_0\end{matrix}\right\} \propto e^{-z/H_0} \qquad (9)$$

$$T_0 = \text{const}$$

and

$$\left.\begin{matrix}\Delta v\\ \\ \Delta w\end{matrix}\right\} \propto \frac{\Delta p}{p_0} \propto e^{-z/\left(\frac{1}{H_1}-\frac{1}{H_0}\right)} \tag{10}$$

The approximate nature of our approach becomes evident by the fact that the condition of an isothermal thermosphere (T_0 = const) and of the exponential decrease with altitude of the heat flux of the wave [$\kappa_0 \Delta T' \propto \exp(-z/H_1)$ in Equation (8)] can not be exactly fulfilled simultaneously in Equations (6). Moreover, within a realistic atmosphere scale height H_0 and collision number ν are height dependent. Therefore, the scale height H_1 of the wave parameters expected to be equal to the scale height H of the heat source has to be considered as an effective value slightly depending on altitude and on the parameters of the thermosphere. From an exact calculation one finds

$$H_0 < H_1 < H.$$

Using Equations (8), (9) and (10) we can derive the following relationship between the different wave parameters from Equations (6):

$$\frac{\Delta p}{p_0} = \alpha \frac{\Delta \rho}{\rho_0}$$

$$\frac{\Delta T}{T_0} = (\alpha - 1) \frac{\Delta \rho}{\rho_0}$$

$$\frac{\Delta v}{c} = -\frac{\alpha S}{\gamma Z} \frac{\Delta \rho}{\rho_0}$$

$$\frac{\Delta w}{c} = j k_0 H_1 \left(1 - \frac{\alpha S^2}{\gamma Z}\right) \frac{\Delta \rho}{\rho_0} \qquad (11)$$

with

$$k_0 = \frac{\omega}{c}$$

$$S = \frac{k_y}{k_0}$$

$$Z = 1 - j \frac{\nu}{\omega}$$

$$\alpha = \frac{H_1}{H_0} > 1$$

$$\frac{p_0}{\rho_0} = \frac{c^2}{\gamma}$$

c = velocity of sound

γ = ratio between the specific heats at constant pressure and at constant volume.

Since the thermosphere is an open system, the external heat Δq_0 absorbed within a sheet at the altitude z_0 generates neutral air waves which re-radiate into the upper and into the lower half space, separated by z_0. Therefore, within the upper half space $z \geq z_0$ only half of the external energy Δq_0 is available to create the observed upgoing density wave. Thus, a factor 1/2 must be added to the external heat source Δq in Equation (6d) in order to meet such radiation condition.

Eliminating now the density amplitude $\Delta\rho$ from Equations (11) and introducing this value into Equation (6d) yields

$$Ze^{j\Phi}\Delta\rho_0 = \Delta q_0 \tag{12}$$

with

$$\bar{Z} = Ze^{j\Phi} = R + j\left(\omega L - \frac{1}{\omega C}\right) \tag{13}$$

and

$$R = R_1 + R_2 = 2\,\frac{\alpha^2 k_y^2 c^4 \nu}{\gamma^2(\omega^2 + \nu^2)} + 2\,\frac{\kappa_0 \Delta T_0'}{H_1 \Delta\rho_0}$$

$$L = \frac{2(\alpha - 1)c^2}{(\gamma - 1)}$$

$$C = \frac{\gamma^2}{2\alpha^2 k_y^2 c^4}\left(1 + \frac{\nu^2}{\omega^2}\right) \tag{14}$$

Comparing Equations (12) and (1) we notice a complete equivalence, if we relate the density amplitude $\Delta\rho_0$ at the height z_0 to an electric current i and the heat input Δq_0 to an electric voltage u, and we can immediately define an atmospheric "inductor" L, "condensor" C and "resistor" R by Equations (14).

From the Equation of energy (6d) we identify the "inductance" L as connected with the internal energy of the wave and with vertical heat convection, the "capacitance" C as connected with horizontal and vertical heat convection and the "resistance" R as connected with ion drag and vertical heat conduction. The

"capacitance" C increases with collision number ν, with decreasing horizontal wave number k_y and with decreasing frequency ω. The ion drag term R_1 of the "resistance" R first increases with ν, reaches a maximum at $\nu = \omega$ and then approaches zero for $\nu \to \infty$, it decreases with ω and increases with k_y. The "inductance" L and the heat conduction term R_2 of R in our approximation remain independent of ω, ν or k_y.

The eigenfrequency of the system according to Equation (4) is

$$\Omega = \frac{\alpha k_y c}{2\gamma} \sqrt{\frac{(\gamma - 1)}{(\alpha - 1)\,(1 + \nu^2/\omega^2)}} \tag{15}$$

However for $k_y \neq 0$ Equation (15) because of the frequency dependence of Ω is not identical with the effective eigenfrequency of the system for which the imaginary part of $\bar{Z}$ vanishes. This effective eigenfrequency is

$$\omega_{eff} = \sqrt{\frac{\alpha^2 k_y^2 c^2 (\gamma - 1)}{4\gamma^2 (\alpha - 1)} - \nu^2} \tag{16}$$

4. NUMERICAL RESULTS

We shall give in this section numerical results of Equation (13). We shall compare these results with exact calculations in order to test the validity of Equation (13) and to find out some basic data about the relationship between density amplitude and heat input depending on frequency, collision number and horizontal wave number. We confine ourselves to a height of $z_0 = 350$ km and use as atmospheric parameters the data of the Jacchia-model (Jacchia, 1964) at an exospheric temperature of $T_\infty = 1000°$ K.

4a. Diurnal Density Variation and its Dependence on Collision Number ν

We first estimate the influence of the collision number ν on the amplitude and phase relationship between diurnal EUV heat input and density. We use the data

$$\omega = 7.28 \times 10^{-5}\ \text{sec}^{-1} \quad ; \quad k_y = 1.5 \times 10^{-4}\ \text{km}^{-1}$$

$$\gamma = 1.5 \quad ; \quad c = 0.84\ \text{km/sec}$$

$$H_0 = 53\ \text{km} \quad ; \quad H = 100\ \text{km} \qquad (17)$$

$$H_1 = 74\ \text{km}$$

$$\alpha = 1.4 \quad ; \quad \frac{\kappa_0 \Delta T_0'}{\Delta \rho_0} = 1.9 \times 10^{-3}\ \text{km}^3/\text{sec}^3$$

and vary ν from 10^{-5} to 10^{-2} sec^{-1}. The result is shown in Figure 2 where "impedance" Z and phase angle Φ [see Equation (13)] are plotted versus ν as full lines. The dashed lines in Figure 2 have been calculated using the exact system of the dynamic equations, taking into account the transmission characteristics of the thermosphere between 100 and 400 km altitude and the height dependence of ν used in (Volland, 1968).

The number $\alpha = H_1/H_0$ in Equation (17) has been selected such that at $z_0 = 350$ km and for $\nu = 4 \times 10^{-4}$ sec^{-1} the results of the exact calculations are in good agreement with the approximate relations in Equation (11). The number $\kappa_0 \Delta T_0' / \Delta \rho_0$ has been chosen in order to find optimal agreement within the whole range of collision number ν and of frequency ω. Actually both numbers slightly

depend on ν and ω. In our approximation we take them as constants. Therefore, we can not expect complete agreement between the exact calculations and our approximation. Nevertheless, as Figure 2 and the following figures indicate, the essential features of the density variation are well reproduced by our approximation.

Figure 2a shows that the "impedance" Z only slightly decreases with the collision number ν. Therefore, the density amplitude generated by the EUV heat source does not depend very much on ν. According to Jacchia (1964) the diurnal density amplitude at 350 km altitude and at moderate solar activity ($\bar{F} = 125$) is

$$|\Delta\rho_0| = 3.3 \times 10^{-15} \text{ g/cm}^3 \tag{18}$$

Therefore the EUV heat input necessary to generate this wave amplitude at 350 km altitude is

$$|\Delta q_0| < Z|\Delta\rho_0| = 5 \times 10^{-9} \text{ erg/cm}^3\text{sec} \tag{19}$$

The "smaller than" sign in Equation (19) takes account of the fact that the density amplitude of Equation (18) is in part generated by a tidal wave from below (Volland, 1968).

The phase delay Φ of the density in Figure 2b varies from -75° to 70° with increasing collision number equivalent to a time advance and a time delay, respectively, with respect to the solar EUV heat source varying from -5 hours to 4,7 hours. The observed time lag of about 2.5 hours in the density maximum therefore corresponds to a collision number of

$$\nu = 4 \times 10^{-4} \text{ sec}^{-1} \tag{20}$$

which is in good agreement with the value derived from Dalgarno's (1964) formula of ν at the height of the maximum of the equatorial F2 layer.

Figure 3a shows the ν-dependence of the "circuit" elements ωL, $1/\omega C$, R_1 and R_2 [see Equation (14)]. In Figure 3b the real part

$$R = R_1 + R_2 \tag{21}$$

and the imaginary part

$$I = \omega L - \frac{1}{\omega C} \tag{22}$$

of the complex impedance

$$\bar{Z} = R + j\, I$$

are plotted versus ν. We notice that with increasing ν, the influence of heat convection (the term $1/\omega C$) decreases, is compensated by the internal heat (the term ωL) at $\omega = \omega_{eff}$ and finally disappears. The phase Φ in turn shifts from

$$\Phi = tg^{-1} \left\{ \frac{\omega}{R_2} \left(\frac{2\alpha^2 c^2 S^2}{\gamma^2} - L \right) \right\}$$

at

$$\nu = 0$$

over

$$\Phi = 0$$

at

$$\nu = \sqrt{\frac{a^2 k_y^2 c^2 (\gamma - 1)}{4\gamma^2 (a - 1)} - \omega^2}$$

to

$$\Phi = tg^{-1}\left\{\frac{\omega_i^L}{R_2}\right\}$$

at

$$\nu \to \infty \tag{23}$$

Resistance R_1 due to ion drag is of the same order of magnitude than heat conduction term R_2 in the range $\nu = \omega$. Outside this range it decreases.

4b. Semidiurnal Tides and Higher Harmonics

The observations of the tidal density variation within the thermosphere clearly gives evidence of the predominance of the diurnal component (Jacchia and Slowey, 1966). This is in contrast to the situation within the lower atmosphere, where the semidiurnal component predominates (see e.g., Siebert, 1961). The reason for the smallness of the diurnal component in the lower atmosphere in spite of its largest excitement by solar radiation as the driving force is due to the fact that this wave mode is of an evanescent type there (Siebert, 1961; Kato, 1966; Lindzen, 1967) so that its propagation is suppressed.

Within the thermosphere the diurnal component changes into a propagation mode (Volland and Mayr, 1968), and its "impedance" Z becomes smaller than

the respective values of the higher harmonics. In order to show this we repeated our calculations taking into account higher harmonics of the local time

$$m\tau = \omega_m t + k_m y \tag{24}$$

with

$$\omega_m = m\omega \quad ; \quad m = 1, 2, 3, 4$$

$$k_m = m\, k_y$$

and plotted "impedance" Z and phase angle Φ versus m in Figure 4. Since the diurnal component of the EUV heat source (exactly speaking the P_{11}-component) is by far the largest component, and, moreover, Z in Figure 4a increases with m, the higher harmonics of the tidal wave are expected to be of no significance within the thermosphere, which is confirmed by the observations.

4c. Geomagnetic Activity Effect, 27 Day Variation and Semiannual Variation of the Thermospheric Density

The geomagnetic activity effect, the 27 day variation and the semiannual effect of the thermospheric density are nearly independent of solar local time (see e.g., Priester et al., 1967). Therefore, they can be treated by a one dimensional model (Volland, 1969b). In our approximation this implies the neglect of horizontal convection ($k_y = 0$). Then according to Equation (14) the influence of horizontal heat convection ($1/\omega C$) and of ion drag (R_1) disappears. Internal energy (the term ωL, which includes a contribution of vertical heat convection) and vertical heat conduction (the term R_2) remain the only energy forms into which external solar EUV heat can be transformed.

In order to show the influence of frequency ω on the excitement of a density wave we calculated Z and Φ as functions of ω using the same parameters as in Equation (17) (see Figure 5, full lines). The phase shifts from zero to about 60° within the frequency range considered and tends to become 90° for very high frequencies. We notice a slow increase of Z with ω. At periods greater than 10 days the "impedance" Z remains nearly constant while the phase angle Φ has dropped to zero. This follows from the decreasing influence of internal heat. It means that in this range of frequency the thermosphere behaves quasistatically and can be treated by the static equation of heat conduction.

The dashed lines in Figure 5 are exact calculations of thermospheric dynamics (Volland, 1969b). The four respective dashed lines in Figure 5 have been calculated taking into account a lower boundary of the heat input at

$$z_{min} = 100,\ 120,\ 150 \text{ and } 200 \text{ km}$$

altitude, respectively. Here we observe the interesting phenomen that the heat input within the lower thermosphere below 200 km altitude becomes of significant influence on the resulting values of Z and Φ at 350 km altitude for periods greater than one solar day. Our approximation is best in agreement with the 150 or 200 km boundary data which means that the density wave, generated by the heat input between 100 and 150 km, is suppressed from propagating upwards at periods

$$\Delta t_0 = \frac{2\pi}{\omega} \lesssim 1 \text{ day}.$$

However, at higher periods the density wave can penetrate into the upper

thermosphere with increasing significance. Such phenomen can be called a thermospheric skin effect.

The vertical bars in Figure 5b indicate the range of observed delay times of the geomagnetic activity effect with respect to the geomagnetic activity factor K_p [5 hours according to Roemer (1967a), 7 hours according to Jacchia et al. (1966)], the delay time of the 27 day variation with respect to the excessive solar flux [1 day according to Roemer (1967b), 2.3 days according to MacDonald (1963)] and of the semiannual effect with respect to the equinox [10 to 20 days according to Jacchia et al. (1968)]. In the case of the geomagnetic activity effect we assumed a quasiperiod of $\Delta t_0 \sim 1.2$ days which is an average impulse time of this effect.

From a comparison between observations and calculations we conclude that during the 27 day variation the penetration of the solar EUV heat into the thermosphere stops at about 120 km altitude to be efficient. However, in the case of the semiannual effect most of the heat is deposited within 100 and 120 km altitude. This heat input is explained as arising from the dissipation of wave energy of the tidal wave from the lower atmosphere, the amplitude of which varies semiannually due to changing prevailing winds within the lower atmosphere (Volland, 1969b). Finally, the heat input which causes the geomagnetic activity effect also is deposited predominantly within the lower thermosphere.

In this connection we notice from Figure 5 that the natural response time of the whole thermosphere with respect to diurnally varying heating is of the order of 5 hours, which is just the value found by Harris and Priester (1962) in their

one-dimensional model of the thermosphere without "second heat source". Comparing Figures 5 and 2 we see that horizontal heat convection is an essential part in the diurnal variation of the thermospheric density.

5. CONCLUSION

Using an approximate approach by neglecting the transmission quality of thermospheric waves the equations of the dynamics of the neutral thermosphere can be transformed in such a way that the equation of conservation of energy formally equals the equation of an electric circuit system. The "electric current" in this system is represented by the density amplitude, while the "electric voltage" is equivalent to the external heat input. The "inductance" of the system is related to internal heat and to vertical heat convection of the thermospheric wave, the "capacitance" is related to horizontal and vertical heat convection and the "resistance" is related to ion drag and vertical heat convection.

In a numerical calculation depending on frequency, collision number and horizontal wave number the behavior of the different "circuit elements" is discussed. The numerical results are compared with results from an exact full wave theory and show sufficient agreement for periods equal or smaller than one solar day. However for larger periods, waves generated within the lower thermosphere below 200 km can propagate upwards and significantly participate in the observed density variations. This behavior can be considered as a thermospheric skin effect.

These calculations are applied to the diurnal and semidiurnal tidal density variations within the thermosphere, to the geomagnetic activity affect, the 27 day

variation and the semiannual effect at thermospheric heights. The ratio between external heat source and density amplitude (the "impedance" of the circuit) and the phase delay between heat source and density maximum are determined and compared with observations.

LITERATURE

Dalgarno, A., Ambipolar diffusion in the F-region, Journ. Atm. Terr. Phys. 26, 939, 1964

Glasford, G. M., Linear analysis of electronic circuits, Addison-Wesley Publ. Comp., Reading Mass., 1965

Harris, I. and W. Priester, Time dependent structure of the upper atmosphere, Journ. Atm. Sci., 19, 286-301, 1962

Jacchia, L. G., Static diffusion models of the upper atmosphere with empirical temperature profiles, Smithsonian Institution, Astrophysical Observatory, Special Report No. 170, Cambridge, Mass., 1964

Jacchia, L. G. and J. W. Slowey, The shape and location of the diurnal bulge in the upper atmosphere, Smithsonian Institution, Astrophysical Observatory, Special Report No. 207, Cambridge, Mass., 1966

Jacchia, L. G., Slowey, J. W. and F. Verniani, Geomagnetic perturbations and upper-atmospheric heating, Smithsonian Institution, Astrophysical Observatory, Special Report No. 218, Cambridge, Mass., 1966

Jacchia, L. G., Slowey, J. W. and I. G. Campbell, Semiannual density variations in the upper atmosphere, 1958 to 1966, Smithsonian Institution, Astrophysical Observatory, Special Report No. 265, Cambridge, Mass., 1968

Kato, S., Diurnal atmospheric oscillation, Journ. Geophys. Res., 71, 3201-3214, 1966

Lindzen, R. S., Thermally driven diurnal tide in the atmosphere, Quart. J. Roy. Meteorol. Soc., 93, 18-42, 1967

MacDonald, G. F. C., The escape of helium from the earth's atmosphere, Rev. Geophys., 1, 305-349, 1963

Priester, W., Roemer, M. and H. Volland, The physical behavior of the upper atmosphere deduced from satellite drag data, Space Sci. Rev., 6, 707-780, 1967

Roemer, M., Geomagnetic activity effect derived from Explorer IX drag data, Phil. Trans. Roy. Soc., A 262, 185-194, 1967 a

Roemer, M., Geomagnetic activity effect and 27 day variation: response time of the thermosphere and lower exosphere, Space Res. VII, p. 1091, North-Holland Publ. Comp., Amsterdam, 1967 b

Siebert, M., Atmospheric tides, Adv. Geophysics, 7, 105-187, 1961

Volland, H., A theory of thermospheric dynamics. Part I: diurnal and solar cycle variations, Document X-621-68-503, GSFC, Greenbelt, Md., 1968

Volland, H., The upper atmosphere as a multiply refractive medium for neutral air motions, to be published in Journ. Atm. Terr. Phys., 1969a

Volland, H., A theory of thermospheric dynamics. Part II: Geomagnetic activity effect, 27 day variation and semiannual variation, Document X-621-69-42, GSFC, Greenbelt, Md., 1969b, (to be published in Planet. Space Sc.).

Volland, H. and H. G. Mayr, On the diurnal tide within the thermosphere,
Document X-621-68-444, GSFC, Greenbelt, Md., 1968

FIGURE CAPTIONS

Figure 1. Block diagram of an electric circuit system in series.

Figure 2. Impedance Z (ratio between external heat source and density amplitude) and phase delay Φ of the density amplitude with respect to the external heat source of the diurnal thermospheric tidal density wave versus collision number ν. Full lines have been calculated using the approximate approach, dashed lines are determined from an exact full wave calculation.

Figure 3. (a) Circuit elements of the atmospheric circuit system.

(b) Real part $R = R_1 + R_2$ and imaginary part $I = \omega L - \frac{1}{\omega C}$ of the complex impedance $\bar{Z}$ of the diurnal thermospheric tidal density wave versus collision number.

Figure 4. Impedance Z and phase delay Φ of the thermospheric tidal density wave depending on the domain number m. (m = 1 : fundamental or diurnal component ; m = 2 : semidiurnal component ; m > 2 : higher harmonics). Full lines have been calculated using the approximate approach, dashed lines are determined from an exact full wave calculation.

Figure 5. Impedance Z and phase delay Φ of a one dimensional thermospheric model ($k_y = 0$) versus angular frequency ω (full lines). The upper scale gives the period (in days) of the waves. The dashed lines have been determined by an exact full wave calculation taking into account

different lower boundaries z_{min} of the external heat input. The vertical bars indicate ranges of observed phase delays of the density amplitude with respect to the supposed heat sources of the geomagnetic activity effect, the 27 day variation and of the semiannual effect.

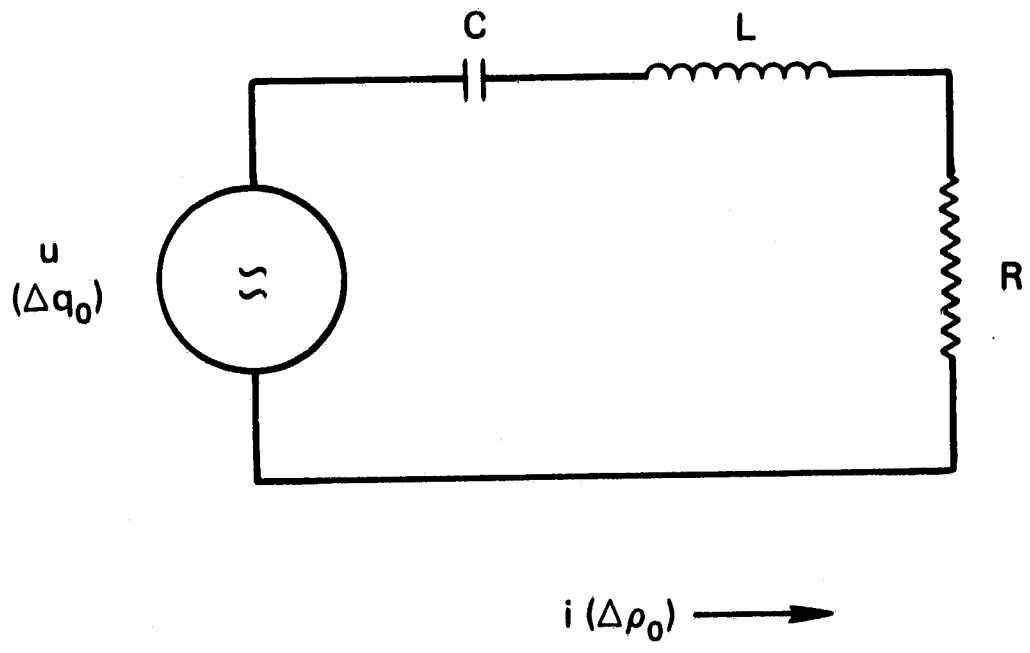

Figure 1. Block Diagram of an Electric Circuit System in Series

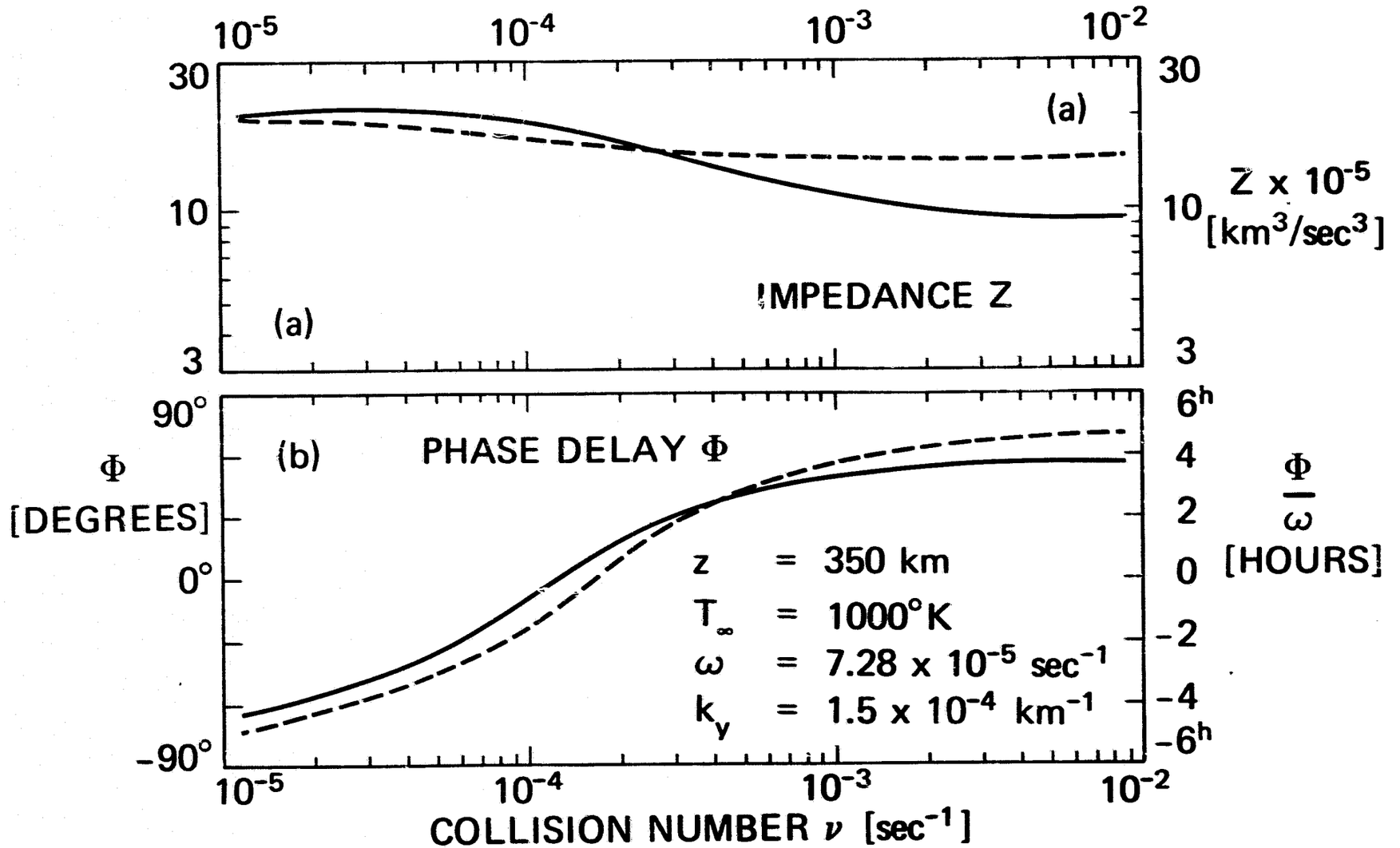

Figure 2. Impedance Z (ratio between external heat source and density amplitude) and phase delay Φ of the density amplitude with respect to the external heat source of the diurnal thermospheric tidal density wave versus collision number ν. Full lines have been calculated using the approximate approach, dashed lines are determined from an exact full wave calculation.

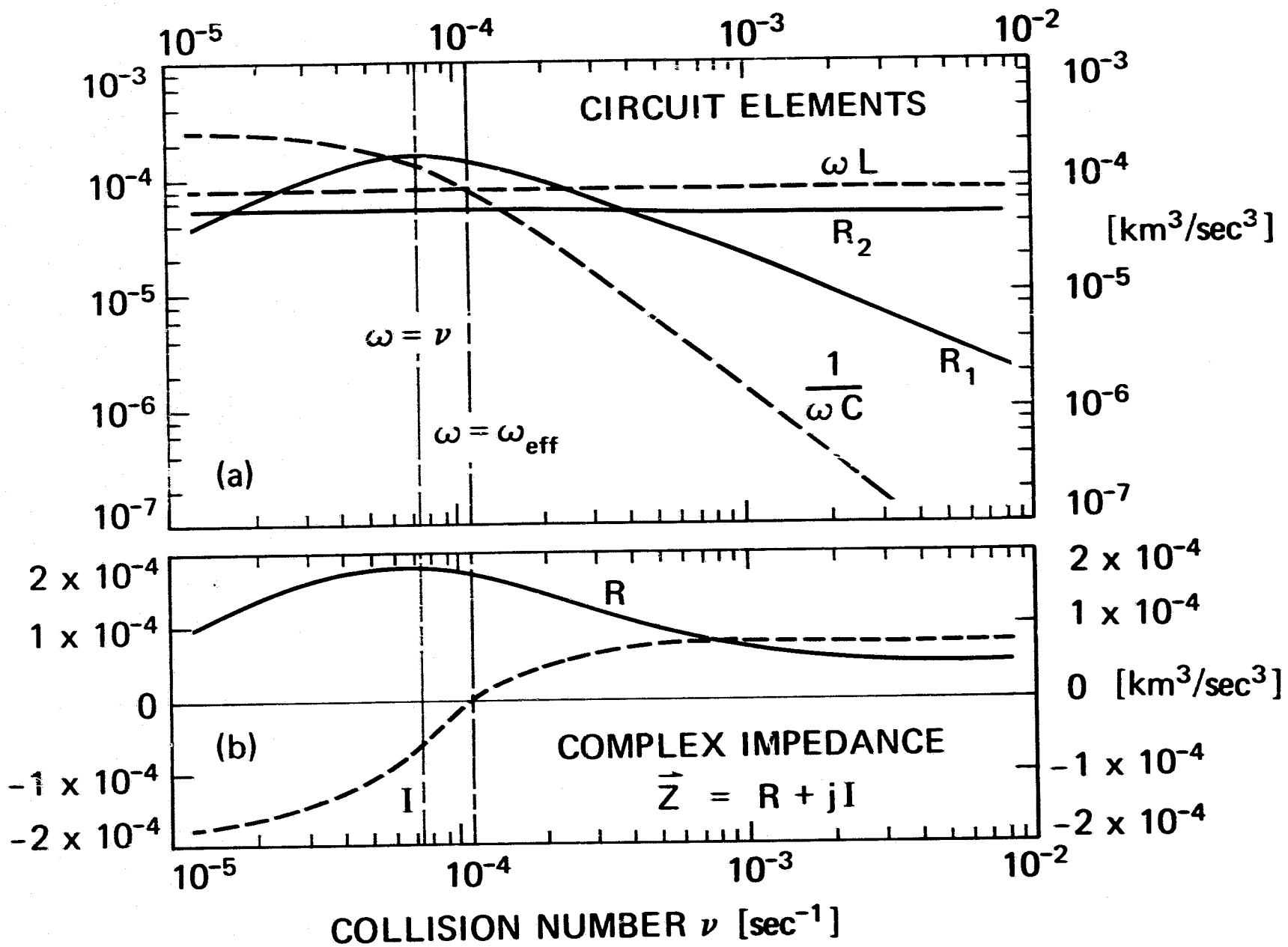

Figure 3. (a) Circuit elements of the atmospheric circuit system. (b) Real part $R = R_1 + R_2$ and imaginary part $I = \omega L - \frac{1}{\omega C}$ of the complex impedance $\bar{Z}$ of the diurnal thermospheric tidal density wave versus collision number.

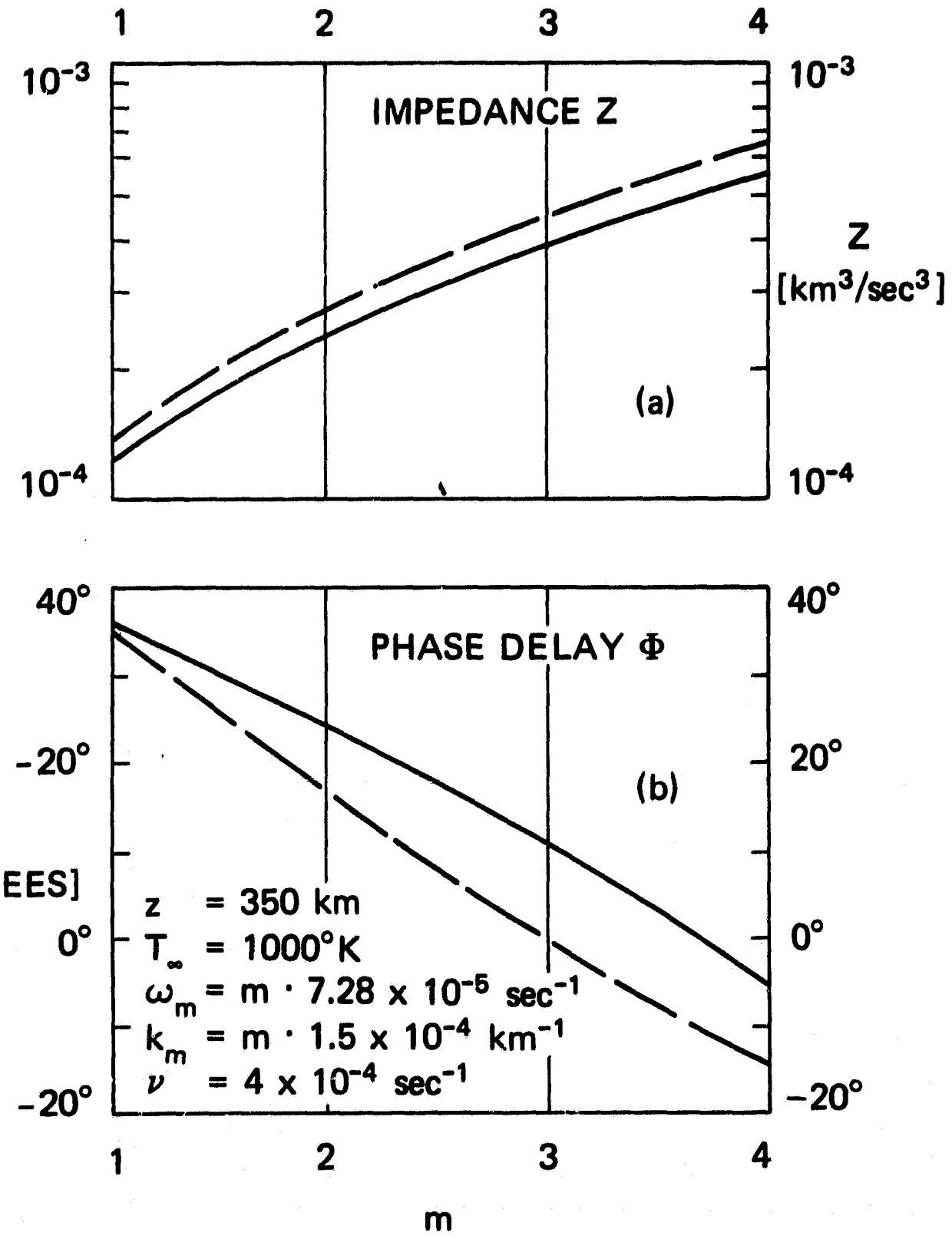

Figure 4. Impedance Z and phase delay Φ of the thermospheric tidal density wave depending on the domain number m. (m = 1 : fundamental or diurnal component ; m = 2 : semidiurnal component; m > 2 : higher harmonics). Full lines have been calculated using the approximate approach, dashed lines are determined from an exact full wave calculation.